Adsorption Modeling with the ESD Equation of State

Aaron D. Soule, Cassandra A. Smith, Xiaoning Yang, and Carl T. Lira*

Department of Chemical Engineering, 2527 Engineering Building, Michigan State University, East Lansing, Michigan 48824

Received March 2, 2000. In Final Form: December 18, 2000

The simplified local density approach (SLD) is extended to the Elliott−Suresh−Donohue (ESD) equation of state for the modeling of gas adsorption on activated carbon, providing significant improvement in quantitative modeling compared to the SLD approach using the Peng−Robinson equation of state or the van der Waals equation. Compared to the Peng−Robinson and van der Waals equations, the ESD equation more accurately represents the temperature dependence of adsorption.

Introduction

Adsorption modeling is an important tool for process simulation and design. Many theoretical models [1,2] have been developed to describe adsorption data for pure substances. Among them are the Langmuir model based on the kinetics approach and the vacancy solution model and two-dimensional equation of state,[3] both of which are based on the thermodynamics approach, along with the other theoretical approaches.[4] The development of modern statistical mechanics theory has driven considerable progress in the application of the density functional theory[5,6] and molecular simulation[7] for adsorption modeling. However, modeling approaches vary depending on the need for computational speed and the desired accuracy of fit. Engineering often desires more rapid methods for obtaining good approximations of adsorption behavior over a wide range of pressures and temperatures. Also, these methods should have a clear physical insight for adsorption phenomena with a set of parameters as few as possible. The Langmuir model, vacancy solution model, and some others are easy to fit, with two to three empirical parameters per isotherm, but require temperature-dependent parameters. Molecular simulation and density functional theories are computationally intensive methods for calculating adsorption. Presently, they are still not available for practical application. Moreover, any theoretical model should also be able to describe the high-pressure adsorption, which shows a maximum in the excess isotherm. Although some theoretical approaches[8−10] have been developed to represent the high-pressure adsorption, they still require temperature-dependent parameters in fitting.

The simplified local density (SLD) approach[11,12] is an engineering method that can be used with any equation of state and offers some predictive capability with only two temperature-independent adjustable parameters for modeling of slit-shaped pores. This paper focuses on results obtained with the Elliott−Suresh−Donohue (ESD) equation of state.

Previous studies have focused on adsorption modeling with the simplified local density approach applied to the van der Waals[11] and Peng−Robinson[12,13] equations of state. These equations, although showing some modeling capabilities, have some characteristics that limit their ability to quantitatively model adsorption in porous materials. For example, the van der Waals equation is the simplest cubic equation and offers only qualitative prediction. The Peng−Robinson equation, on the other hand, represents adsorption of a supercritical fluid such as ethane accurately on flat surfaces. It is capable of predicting the isotherm crossovers above the critical pressure found in experimental data.[12] In porous materials, some success has been obtained,[13] but the temperature dependence of adsorption is typically too weak. For example, Figure 1 shows the application of the SLD model with the Peng−Robinson equation for adsorption of ethylene[14] on BPL carbon. After fitting the isotherm at 301.4 K, the isotherms at 260.2 and 212.7 K are not predicted well.

The ESD equation[16] is also a cubic equation of state; however, its theoretical grounding is superior in that the repulsive term is constructed to match computer simulations of spheres and chains by using a scalar shape factor to account for deviations from spherical geometry. The attractive term consists of an expression for the spherical square-well potential coupled with a shape factor correction. The improved subdivision of repulsive and attractive forces is important for the SLD approach that may lead to the greater accuracy of adsorption modeling.

Simplified Local Density Model Using ESD

The ESD equation of state[15] consists of repulsive and attractive terms which are weighted differently than those in the Peng−Robinson equation of state. The ESD equation

* To whom correspondence should be addressed. Tel: (517) 355-9731. Fax: (517) 432-1105. E-mail: lira@egr.msu.edu.

(1) Yang, R. T. *Gas Separation by Adsorption Processes*; Butterworths: Boston, 1987.
(2) Tien, C. *Adsorption Calculations and Modeling*; Butterworths: Boston, 1994.
(3) Zhou, C.; Hall, F.; Gasem, K. A.; Robinson, R. L. *Ind. Eng. Chem. Res.* **1994**, *33*, 1280.
(4) Riazi, M.; Khan, A. R. *J. Colloid Interface Sci.* **1999**, *210*, 309.
(5) Balbuena, P. B.; Gubbins, K. E. *Langmuir* **1993**, *9*, 1801.
(6) Pan, H.; Ritter, J. A.; Balbuene, P. B. *Ind. Eng. Chem. Res.* **1998**, *37*, 1159.
(7) Gusev, Y. V.; O'Brien, J. A. *Langmuir* **1997**, *13*, 2815.
(8) Malbrunot, P.; Vidal, D.; Vermesse, J. *Langmuir* **1992**, *8*, 577.
(9) Benard, P.; Chahine, R. *Langmuir* **1997**, *13*, 808.
(10) Zhou, L.; Zhou, Y.; Li, M.; Chen, P.; Wang, Y. *Langmuir* **2000**, *16*, 5955.
(11) Rangarajan, B.; Lira, C. T.; Subramanian, R. *AIChE J.* **1995**, *41*, 838.
(12) Subramanan, R.; Pyada, H.; Lira, C. T. *Ind. Eng. Chem. Res.* **1995**, *34*, 3830.
(13) Chen, J.; Tan, C.; Wong, D.; Lira, C. T.; Subramanian, R.; Orth, M. *Ind. Eng. Chem. Res.* **1997**, *36*, 2808.
(14) Reich, R.; Ziegler, W. T.; Rogers, K. A. *Ind. Eng. Chem. Process Des. Dev.* **1980**, *19*, 336.
(15) Elliott, J. R.; Suresh, S. J.; Donohue, M. D. *Ind. Eng. Chem. Res.* **1990**, *29*, 1476.

10.1021/la000311n CCC: $20.00
Published on Web 04/21/2001

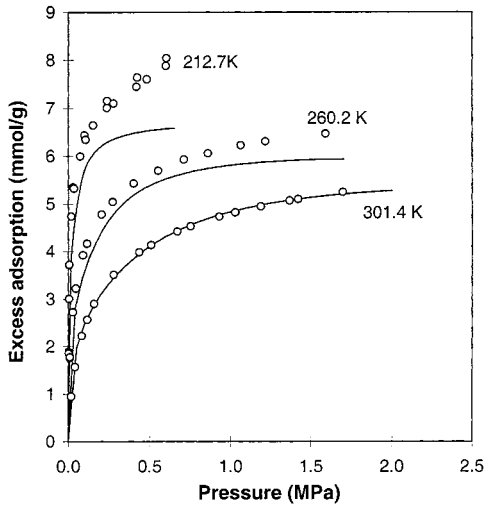

Figure 1. Ethylene isotherms using the Peng−Robinson SLD model with a slit width of $H = 14.2$ Å and $\epsilon_{fs}/k = 110$ K on BPL activated carbon. The data at 301.4 K is fitted, and the other isotherms are predicted based on the fit. Data of Reich et al. (ref 14).

takes the form $Z = 1 + Z^{rep} + Z^{attr}$, where

$$Z^{rep} = \frac{4c\eta}{1 - 1.9\eta} \tag{1}$$

$$Z^{attr} = \frac{9.5q\eta Y}{1 + 1.7745\langle \eta Y\rangle} \tag{2}$$

Here, Z is a compressibility factor, c is a shape factor for the repulsive term, q is a shape factor for the attractive term, η is the reduced density ($\eta = b\rho$), b is the component's size parameter, ρ is the molar density, and Y is a temperature-dependent attractive energy parameter ($Y = \exp(\epsilon/kT) - 1.0617$). Details of the parameters are in the reference cited above. Although the ESD equation also can represent associating fluids, none of the components presented in this paper have associative characteristics, so the associating term is omitted from this paper. The equation can also be represented in terms of fugacity:

$$\ln f = -\frac{4}{1.9}c\ln(1 - 1.9\eta) + \frac{4c\eta}{(1 - 1.9\eta)} - \frac{9.5q}{1.7745}\ln(1 + 1.7745\langle Y\eta\rangle) - \frac{9.5qY\eta}{(1 + 1.7745\langle Y\eta\rangle)} - \ln\frac{V}{RT} \tag{3}$$

where V is the molar volume, T is temperature, R is the ideal gas constant, and f is fugacity.

In the slit-shaped pores used in modeling (see Figure 2), the fluid−solid interaction potential is modeled using the same 10−4 potential[16] as in previous work,[13] incorporating five carbon layers. The potential with one wall is

$$\psi_1(z) = 4\pi\rho_{atoms}\sigma_{fs}^2\epsilon_{fs}\left(\frac{0.2}{\mathrm{Eta}^{10}} - \frac{0.5}{\mathrm{Eta}^4} - \frac{0.5}{(\mathrm{Eta} + \alpha)^4} - \frac{0.5}{(\mathrm{Eta} + 2\alpha)^4} - \frac{0.5}{(\mathrm{Eta} + 3\alpha)^4} - \frac{0.5}{(\mathrm{Eta} + 4\alpha)^4}\right) \tag{4}$$

where $\alpha = 3.35$ Å$/\sigma_{fs}$ is the ratio of the plane spacing between the solid particles divided by σ_{fs}, σ_{fs} is the average value of the fluid and solid molecular diameters [$\sigma_{fs} = (\sigma_{ff} + \sigma_{ss})/2$], z is the particle position in the slit relative to the carbon surface, $\mathrm{Eta} = (z + 0.5\sigma_{ss})/\sigma_{fs}$ is the dimensionless distance from the carbon centers in the first plane (see Figure 1), and ρ_{atoms} represents the number of carbon-plane atoms per square angstrom[16] (0.382 atoms/Å^2). The fluid−solid potential in relation to the second wall, $\Psi_2(z)$, can be calculated by replacing Eta in eq 4 with Xi, which is the distance from the second wall divided by the fluid−solid diameter. The total fluid−solid potential is expressed as

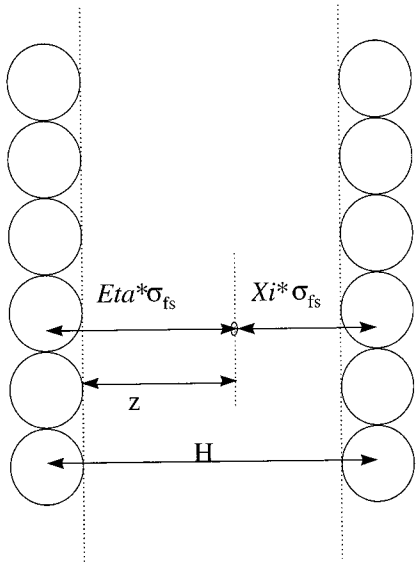

Figure 2. Schematic of a slit-shaped pore model showing the variables used to define distances in the SLD approach; $\mathrm{Eta} = (z + 0.5\sigma_{ss})/\sigma_{fs}$ and $\mathrm{Xi} = (H - \mathrm{Eta}(\sigma_{fs}))/\sigma_{fs}$.

$$\psi_T(z) = \psi_1(z) = \psi_2(z) \tag{5}$$

The thermodynamic constraints of the adsorbing fluid fugacity are represented by eqs 6−8 below.[11−13]

$$\mu_{bulk}[T,\rho_{bulk}] = \mu_{ff}[T,\rho(z)] + \mu_{fs}[z] \tag{6}$$

$$\mu_{ff}[T,\rho(z)] = \mu^0[T] + RT\ln\left\{\frac{f_{ff}[T,\rho(z)]}{f^0[T]}\right\} \tag{7}$$

$$\mu_{bulk}[T,\rho_{bulk}] = \mu^0[T] + RT\ln\left\{\frac{f_{bulk}[T,\rho_{bulk}]}{f^0[T]}\right\} \tag{8}$$

In these equations, μ_{bulk} is the bulk chemical potential, f^0 and μ^0 are the standard state fugacity and chemical potential, respectively, and μ_{fs} is the fluid−solid contribution to the chemical potential ($\mu_{fs} = N_A\psi_T(z)$), where N_A is Avogadro's number. The local chemical potential due to fluid−fluid interactions is designated by μ_{ff} and dependent on T and local density $\rho(z)$. Note that μ_{ff}, μ_{fs}, and f_{ff} are functions of z (position), but μ_{bulk}, μ^0, and f^0 are not. On the basis of the above equations, an expression for f_{ff} can be derived,

$$f_{ff}[T,\rho(z)] = f_{bulk}[T,\rho_{bulk}]\exp\left[\frac{-\psi_T(z)}{kT}\right] \tag{9}$$

Because f_{bulk} is independent of position in the pore and ψ_T is dependent on position only, the local fugacity f_{ff} can be calculated. Then, the local volume (or density) can be

(16) Lee, L. L. *Molecular Thermodynamics of Non-Ideal Fluids*; Butterworths: Boston, 1988; p 425.

Table 1. Pure Component ESD Parameters[17] and Lennard-Jones[18] Size Parameters

component	C	q	ϵ/k (K)	b (cm^3/mole)	σ_{ff} (Å)
acetylene	1.6808	2.2967	190.510	13.053	4.033
n-butane	1.7025	2.338	260.583	29.039	4.687
carbon dioxide	1.8321	2.585	178.269	10.534	3.941
carbon monoxide	1.2367	1.4509	103.784	10.171	3.690
ethane	1.3552	1.6765	220.449	16.716	4.443
ethylene	1.305	1.581	210.275	15.013	4.163
methane	1.0382	1.0728	178.082	10.863	3.758
nitrogen	1.1433	1.273	106.155	9.907	3.798
propane	1.5481	2.0441	241.433	22.921	5.118
propylene	1.5142	1.9794	241.896	20.890	4.678

calculated from a local form of eq 3 which is obtained by modifying the attractive equation of state parameter as explained next.

For previous work[13] with the Peng−Robinson equation, algebraic expressions were developed for the Peng−Robinson f_{ff} based on the attractive equation of state parameter, $a(z)/a_{bulk}$. As explained in previous work, the fluid−fluid interactions depend on the geometry and position within the pore, and equations for $a(z)/a_{bulk}$ are presented in that publication. The same expressions are used in this work in order to calculate the ESD $Y(z)/Y_{bulk}$ because parameter Y in the ESD equation of state takes the same role as the parameter a in the Peng−Robinson equation. Thus, in slits, the local fluid−fluid chemical potential (fugacity) is calculated from Y_{bulk} and the algebraic expressions for $Y(z)/Y_{bulk}$, which is the same form as $a(z)/a_{bulk}$ in the ref 13 except as noted in the next paragraph. Substituting $f_{ff}[T,\rho(z)]$ for the left side of eq 3 and substituting $Y(z)$ for Y on the right side yields an equation that can be solved for $\rho(z)$ (i.e., $1/V(z)$).

In previous work, fluid closer to the wall than $z/\sigma_{ff} = 0.5$ was ignored.[13] To provide a more realistic density profile near the wall, this work assumes that the density cutoff should be the point where the local fugacity, f_{ff}, is $^1/_{10}$ of a percent of the bulk fugacity, f_{bulk}. From eq 9, one can calculate $\Psi(z)/k$ as approximately 2500 K when $f_{ff}/f_{bulk} = 0.001$ at 373 K. This value of $\Psi(z)/k$ is used for all temperatures of this study which makes the cutoff distance dependent on the slit width only. This is an arbitrary but accurate approximation, because the fluid density is negligible closer to the wall in all calculations we have checked. The functions for $Y(z)/Y_{bulk}$ are derived for $z/\sigma_{ff} \geq 0.5$. For the calculations in the slit region closer to the surface wall than $0.5\sigma_{ff}$, we choose to use the value of $Y(z)/Y_{bulk}$ at $z/\sigma_{ff} = 0.5$. This approximation of the $Y(z)/Y_{bulk}$ function will have a negligible effect in this region because the fluid density goes to zero rapidly nearer the wall.

The local density is obtained at each z by using eqs 3, 4, 5, and 9. The difference between the local and bulk densities is integrated in the correct geometric form over the entire slit width using the modified Simpson's rule to yield excess adsorption, Γ^{ex}.

$$\Gamma^{ex} = \frac{A}{2}\int_{z=0}^{z \text{ at far wall}} [\rho(z) - \rho_{bulk}]\, dz \qquad (10)$$

The variable A is the surface area per unit weight of adsorbent (e.g., square meters per gram). In the case of adsorption in a slit with homogeneous parallel walls, the integration over the entire slit width is divided by 2 because two walls contribute to the surface area of a slit.

For each fit discussed in this paper, the value of A was taken from the cited reference and not used as an adjustable parameter in the model. Table 1 lists the pure component ESD parameters,[17] all of which are obtained from bulk fluid properties and were unadjusted in this study. The values of σ_{ff} are tabulated Lennard-Jones diameters of each fluid,[18] and $\sigma_{ss} = 3.4$ Å is the reported diameter of carbon.[5,16] In calculating adsorption in slits, two adjustable temperature-independent parameters were fitted: ϵ_{fs}/k (fluid−solid interaction potential in Kelvin) and H (slit width in angstroms). The parameter H determines the upper limit of eq 10. Except as noted in the captions, the parameters were fit to optimize the simultaneous representation of all data in a given figure rather than optimization of individual isotherms.

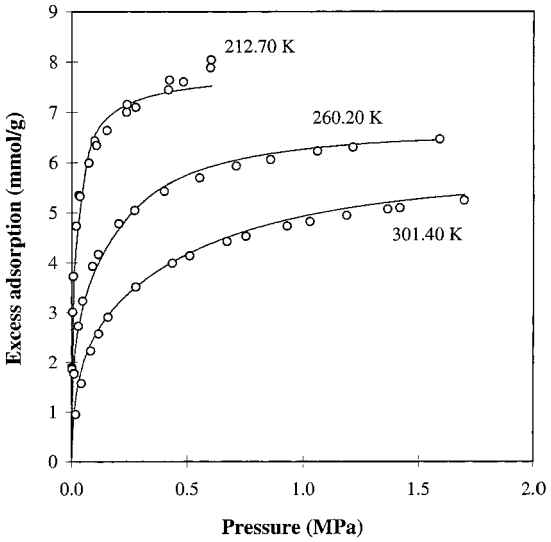

Figure 3. Adsorption of ethylene on BPL activated carbon (988 m^2/g) where $H = 13.7$ Å and $\epsilon_{fs}/k = 103$ K. The isotherm at 301.4 K is fitted, and the other two isotherms are predicted. Data of Reich at al. (ref 14).

Results and Discussion

Several sets of pure component adsorption data have been successfully fitted with the ESD version of the simplified local density model. In the following figures, the points give the experimental data, and the lines give the fitting results. Figures 3 and 4 show the adsorption of ethylene on BPL carbon[14,19] over a 167 K temperature range. Figures 5 and 6 show ethane adsorption,[14,19] which is also a good fit over a 167 K temperature range. Other fits include butane[19] over 110 K (Figure 7), propane[19] over 167 K (Figure 8), methane[14] over 89 K (Figure 9), propylene[19−21] over 139 K (Figures 10, 11, and 12) and nitrogen[19] over 111 K (Figure 13). Except for Figure 3, all fits were performed by simultaneously optimizing the fit for all of the isotherms in a given graph through adjustment of two parameters. All adjustable parameters used to fit the isotherms are given in the figure captions. The model does a good job of representing the temperature dependence of the isotherms without temperature-dependent parameters.

The ethylene isotherm shape at 212.7 K (Figure 3) is not represented as accurately as the higher temperature isotherms. This is because the isotherm approaches

(17) Elliott, J. R.; Lira, C. T. *Introductory Chemical Engineering Thermodynamics*; Prentice Hall: Upper Saddle River, NJ, 1999.
(18) Reid, R. C.; Prausnitz, J. M.; Poling, B. E. *The Properties of Gases and Liquids*, 4th ed.; McGraw-Hill: New York, 1987.
(19) Ray, G. C.; Box, E. O. *Ind. Eng. Chem.* **1950**, *42*, 1315.
(20) Laukhuf, W. L. S.; Plank, C. A. *J. Chem. Eng. Data* **1969**, *14*, 48.
(21) Lewis, W. K.; Gilliland, E. R.; Chertow, B.; Hoffman, W. H. *J. Am. Chem. Soc.* **1950**, *72*, 1153.

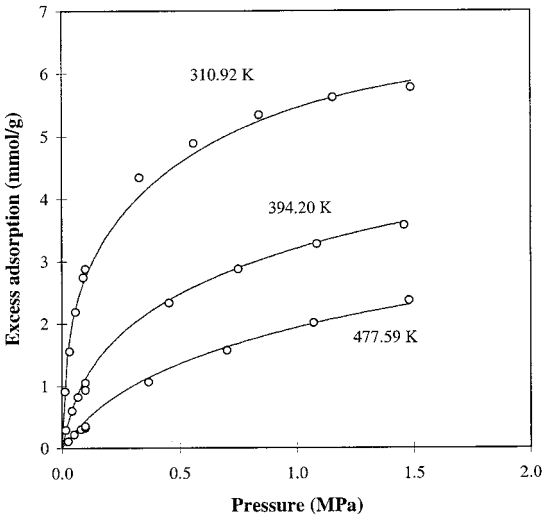

Figure 4. Adsorption of ethylene on Columbia Grade L carbon (1152 m^2/g) where $H = 13.7$ Å and $\epsilon_{fs}/k = 104$ K. Data of Ray and Box (ref 19).

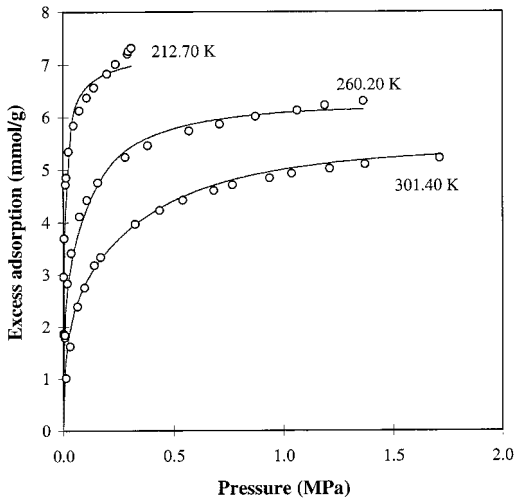

Figure 5. Adsorption of ethane on BPL activated carbon (988 m^2/g) where $H = 14.2$ Å and $\epsilon_{fs}/k = 102$ K. Data of Reich et al. (ref 14).

ethylene's vapor pressure (0.74 MPa) and the fluid begins to exhibit condensation on the exterior surfaces of the particles, which is not represented by the porous model discussed here. The external surface area exhibits layer formation as the vapor pressure is approached.[11] The observed behavior might be modeled by a combination of porous surface area and flat wall surface area. The ethane isotherm at 212.7 K (Figure 5) exhibits the same behavior as the ethylene isotherm at 212.7 K for the same reasons, and thus the shape is not represented as well.

The *n*-butane data of Figure 7 are not simultaneously represented well in the knee region. The slope of the isotherm in the low-pressure region depends on ϵ_{fs}/k. The value of ϵ_{fs}/k needs to have temperature dependence to represent these data better. Increasing the value of ϵ_{fs}/k results in a higher Henry's Law constant and a more rapid rise in the isotherm at low pressure. To represent these data better, ϵ_{fs}/k should decrease with temperature. The fits of propane and propylene could also be improved if ϵ_{fs}/k is allowed to be temperature-dependent, but the theoretical justification depends on whether the nonspherical geometry can justify such an approach.

Nitrogen, methane, acetylene[19] (Figure 14), carbon dioxide[14] (Figure 15), and carbon monoxide[19] (Figure 16)

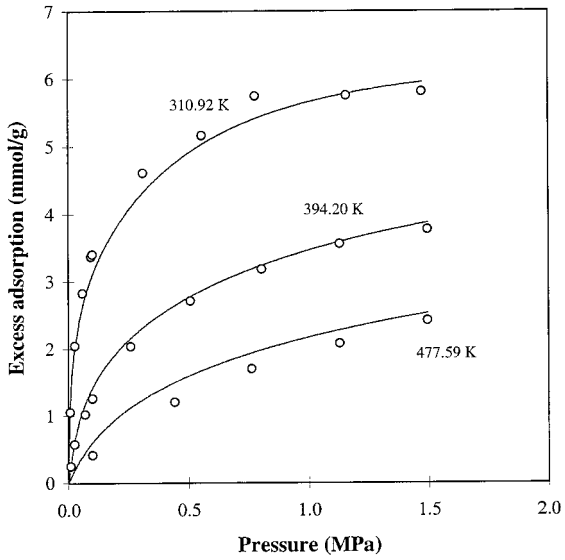

Figure 6. Adsorption of ethane on Columbia Grade L carbon (1152 m^2/g) where $H = 14.3$ Å and $\epsilon_{fs}/k = 104$ K. Data of Ray and Box (ref 19).

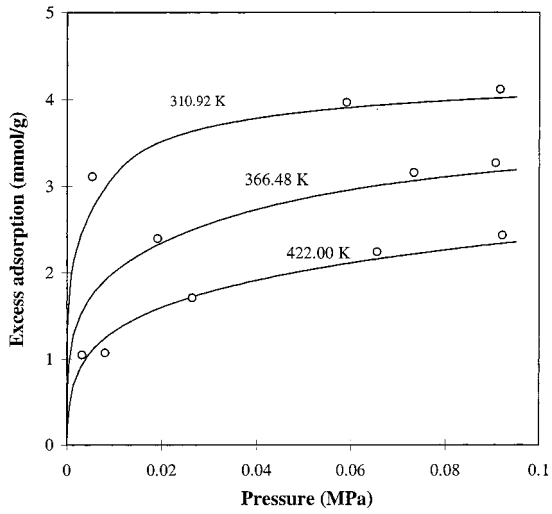

Figure 7. Adsorption of butane on Columbia Grade L carbon (1152 m^2/g) where $H = 14.0$ Å and $\epsilon_{fs}/k = 158$ K. Data of Ray and Box (ref 19).

all are fit well without temperature-dependent parameters. C3 and C4 gases are not represented as well. The Lennard-Jones diameter parameter for propane seems large compared with others from the same source, which may be a factor in the larger slit size needed for propane in the model. The data for these compounds is also generally below 1 bar. Another factor is that although the ESD equation of state is developed to consider shape, the current SLD approximation uses the same shape factor as the bulk fluid and assumes that the fluid−fluid interactions are spherically symmetric in the derivation of $Y(z)/Y_{bulk}$. This approximation may not be good near the surface of the wall for linear adsorbates, which may be a contributing factor to the need for temperature dependence in ϵ_{fs}/k for these higher molecular weight substances. An improved method to incorporate shape into the SLD near the wall may improve temperature dependence of adsorption modeling without requiring temperature-dependent ϵ_{fs}/k.

High-pressure adsorption data, which show some maximum in the excess isotherms, are also fitted by the ESD−SLD model in this work. Figures 17 and 18 give the results for carbon dioxide[13,21] on two different activated

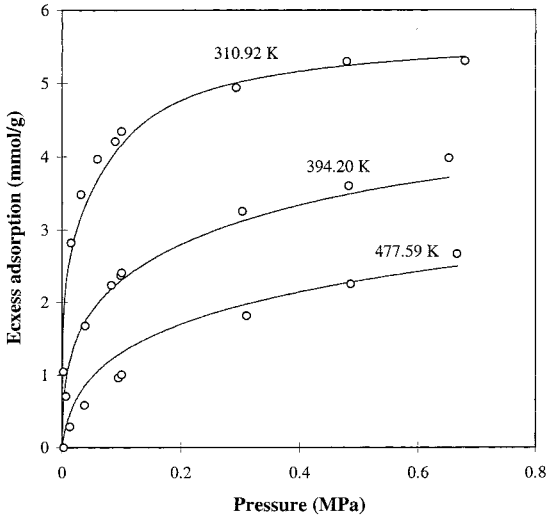

Figure 8. Adsorption of propane on Columbia Grade L activated carbon (1152 m^2/g) where $H = 15.6$ Å and $\epsilon_{fs}/k = 114$ K. Data of Ray and Box (ref 19).

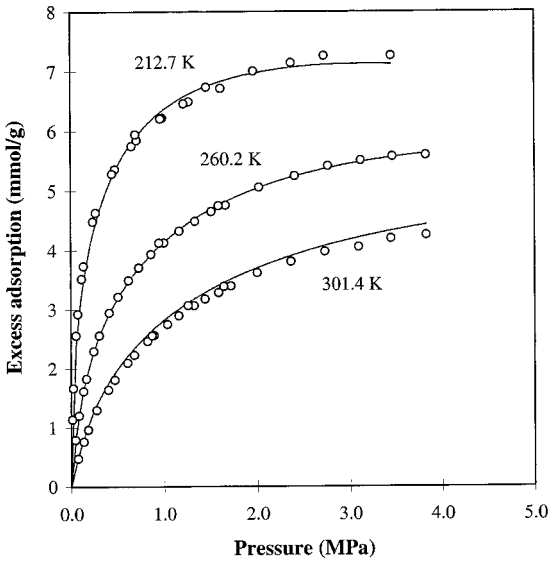

Figure 9. Adsorption of methane on BPL activated carbon where $H = 12.1$ Å and $\epsilon_{fs}/k = 73$ K. Data of Reich et al. (ref 14).

carbons for pressures up to 16 MPa. A crossover phenomenon has been represented by this model above the critical pressure. Figure 19 shows that fitting result for methane adsorption[10] on activated carbon over the temperature range of 233.15−333.15 K. A good agreement is obtained between the experimental measured data and the model fitting. This model reasonably describes the high-pressure maximum observed in the excess isotherms with two temperature-independent parameters.

There is a correlation between the pure fluid Lennard-Jones parameters (ϵ_{ff}/k) from the literature[18] and fluid−solid interaction energy parameters (ϵ_{fs}/k) fitted to isotherms in this work. Figure 20 demonstrates a rough linear relationship between ϵ_{fs}/k and $\sqrt{\epsilon_{ff}/k}$ for Columbia Grade L and BPL carbons. The fluid−solid parameters do show some minor variation between different activated carbons for the same adsorbate, but this effect is small compared to the trend of Figure 20. The fluid−solid interaction energy parameter usually can be estimated by using the Lorentz−Berthelot (L−B) combination rule ($\epsilon_{sf}/k = \sqrt{\epsilon_{ff}/k \cdot \epsilon_{c-c}/k}$), where ϵ_{c-c}/k is the carbon−carbon interaction parameter. This estimation has been extensively used in molecular simulation and density functional approach-

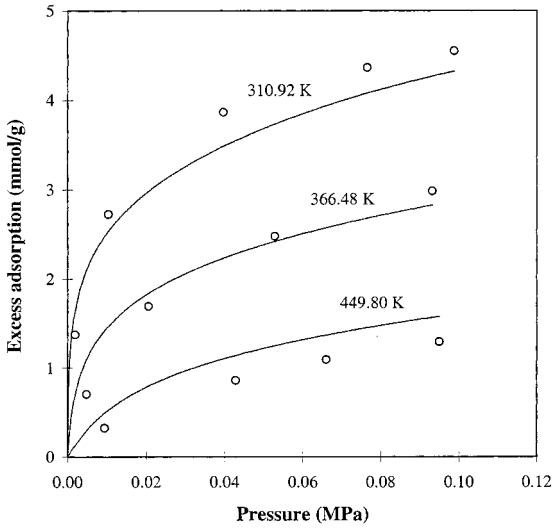

Figure 10. Adsorption of propylene on Columbia Grade L carbon (1152 m^2/g) where $H = 14.1-14.6$ Å (insensitive to H) and $\epsilon_{fs}/k = 126$ K. Data of Ray and Box (ref 19).

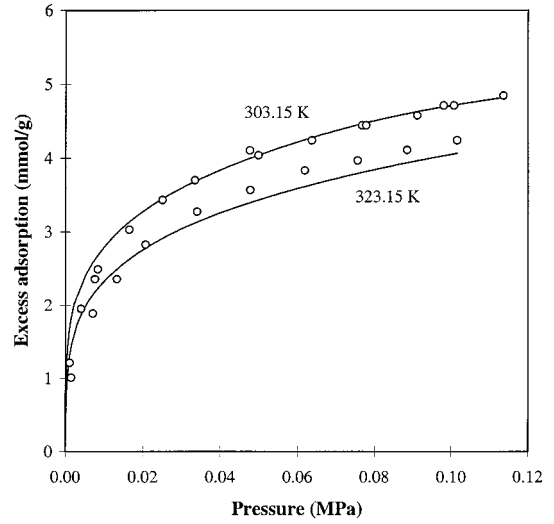

Figure 11. Adsorption of propylene on BPL activated carbon (1100 m^2/g) where $H = 14.1-14.6$ Å (insensitive to H) and $\epsilon_{fs}/k = 132$ K. Data of Laukhuf and Plank (ref 20).

es.[5−7] The estimated values for ϵ_{fs}/k with the L−B combination rule (using $\epsilon_{c-c}/k = 28$ K)[5−7] are also given in Figure 20 for comparison. As seen in Figure 20, the fitted fluid−solid interaction parameters ϵ_f/k in this work are higher than those from the L−B rule. This deviation is more apparent for the bigger molecules. A possible explanation is that the L−B combination rule is only approximate and is more suitable for simple molecules, whereas the heavier components usually possess the multicenter interactions together with other electrostatic interactions (such as dipole−dipole, etc.). So, the adjustable interaction parameter obtained in this model may be thought as an effective parameter involving all these effects.

There is some variation of the slit width (H) among the fits for the various adsorbates. A slit width near 14 Å fits most isotherms except for propane (15.6 Å) and methane (12.1 Å). The reason for the deviations of the modeled slit width for these fluids is as follows. As is well-known, there is a pore size distribution for micropore adsorbents; thus, the adjustable parameter of slit width in this model should be considered as a mean slit size in a broad sense. Studies have shown that different gas probes may obtain different

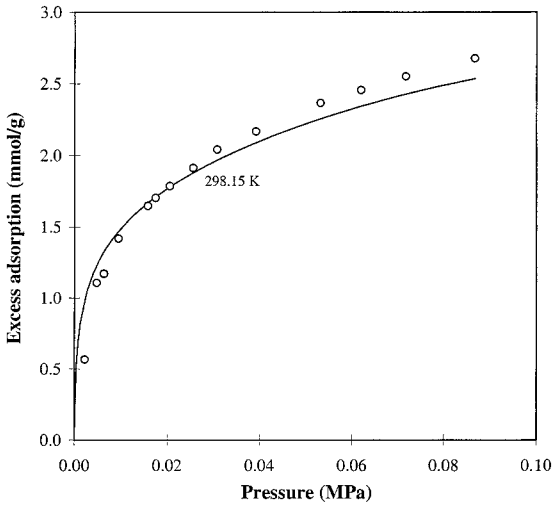

Figure 12. Adsorption of propylene on Black Pearls I carbon (705 m^2/g) where $H = 14.0-14.5$ Å (insensitive to H) and $\epsilon_{fs}/k = 115$ K. Data of Lewis et al. (ref 21).

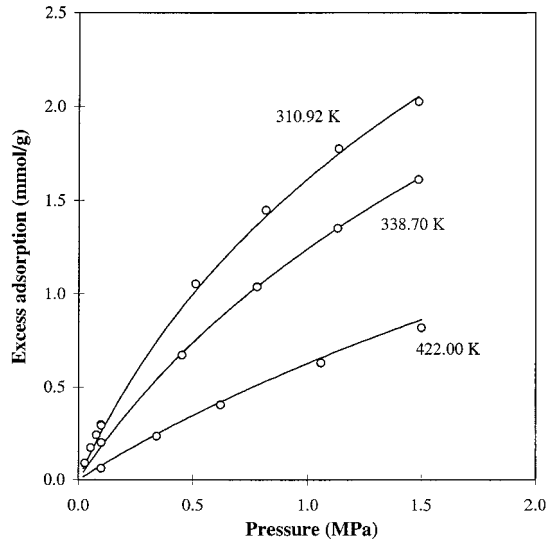

Figure 13. Adsorption of nitrogen on Columbia Grade L carbon (1152 m^2/g) where $H = 14.6$ Å and $\epsilon_{fs}/k = 60$ K. Data of Ray and Box (ref 19).

pore size distributions.[23,24] So, the mean slit sizes from different adsorption substances may be different. Another factor may be the ESD representation of densities within the slits.

When examining the ESD equation of state, it is also important to consider the accuracy of the bulk property calculations. Because the adsorbed phases have liquidlike densities, the representation of liquid molar volumes is important. Table 2 gives some saturation bulk property comparisons between the Peng–Robinson and ESD equations[17] and experimental data[25] near each component's critical temperature calculated with available software.[17] This particular sample of bulk properties was chosen to give the reader a general perspective on the performance of the ESD as compared to experimental data and the

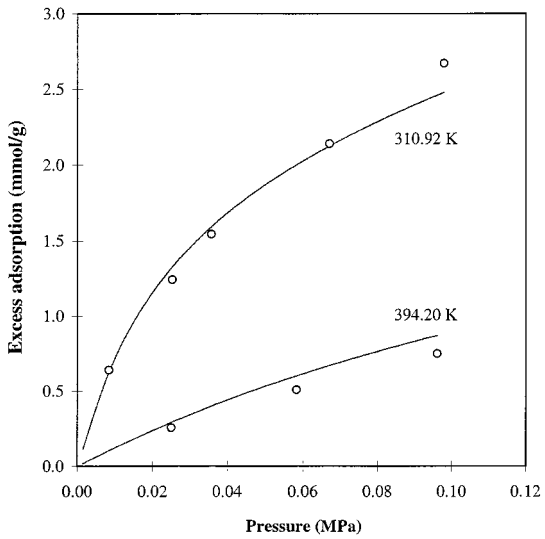

Figure 14. Adsorption of acetylene on Columbia Grade L carbon (1152 m^2/g) where $H = 13.9-14.5$ Å (insensitive to H) and $\epsilon_{fs}/k = 100$ K. Data of Ray and Box (ref 19).

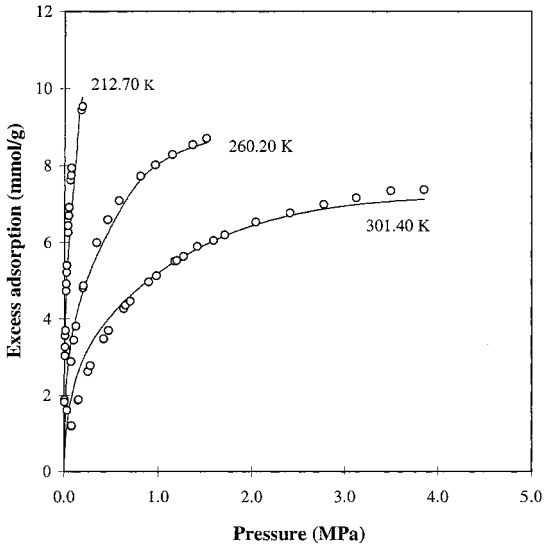

Figure 15. Carbon dioxide adsorption on BPL carbon (988 m^2/g) where $H = 14.2$ Å and $\epsilon_{fs}/k = 99$ K. Data of Reich et al. (ref 14).

Peng–Robinson equation of state. Although the ESD appears to predict gas volumes better than the Peng–Robinson equation, the ESD is weaker in predicting liquid properties. As can be seen in the data, the ESD volumes vary from experimental volumes by 20% or more for liquids. Gas volumes vary by up to 10%. The ability of the ESD to more accurately model adsorption over wide temperature ranges is attributed to the superior representation of the individual contributions of attractive and repulsive forces, because the bulk liquid properties are predicted with about the same or less accuracy.

Summary

This paper has shown that the ESD equation of state can be adapted for successful adsorption modeling. Although the higher molecular weight components presented in this paper cannot be fitted as well as others, it is important to note that good engineering approximations can still be made with any of these compounds.

(22) Ozawa, S.; Kusumi, S.; Ogino, Y. In *Proceedings of the Fourth International Conference on High Pressure*, Kyoto, Japan, 1974.
(23) Scaife, S.; Kluson, P.; Quirke, N. *J. Phys. Chem. B* **2000**, *104*, 313.
(24) Heuchel, M.; Davies, G. M.; Buss, E.; Seaton, N. A. *Langmuir* **1999**, *15*, 8695.
(25) Starling, K. E. *Fluid Thermodynamic Properties for Light Petroleum Substances*; Gulf Publishing Co.: Houston, TX, 1973.

Table 2. Comparison of Experimental Saturation Molar Volumes[25] to the Bulk Peng−Robinson and Bulk ESD Predictions[17] [a]

	temperature (K)	reduced temp	pressure (MPa)	experimental $cm^3/gmol$	Peng−Robinson $cm^3/gmol$	ESD $cm^3/gmol$
methane (L)	188.7	0.99	4.32	70.12	83.30	91.84
methane (G)				162.51	153.74	160.48
ethane (L)	302.6	0.99	4.62	102.44	121.00	134.00
ethane (G)				235.98	217.18	231.33
propane (L)	363.7	0.98	3.81	143.94	155.28	175.33
propane (G)				368.35	356.55	382.21
n-butane (L)	422	0.99	3.62	213.63	219.00	247.39
n-butane (G)				371.86	379.11	414.71
ethylene (L)	277.6	0.98	4.51	86.88	101.23	113.41
ethylene (G)				240.70	231.54	245.65
propylene (L)	360.9	0.99	4.29	131.62	152.18	172.04
propylene (G)				300.22	298.49	321.69
nitrogen (L)	124.8	0.99	3.17	63.80	74.36	81.28
nitrogen (G)				146.31	140.28	147.06

[a] All data points are near the critical temperature.

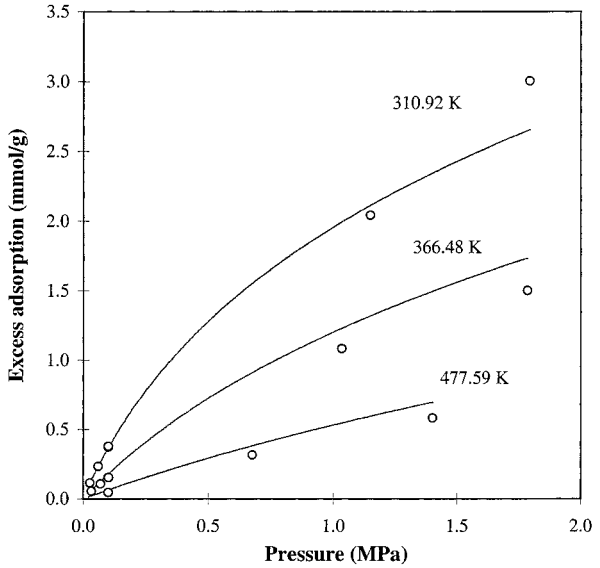

Figure 16. Adsorption of carbon dioxide on Columbia Grade L carbon (1152 m^2/g) where $H = 15.8$ Å and $\epsilon_{fs}/k = 70$ K. Data of Ray and Box (ref 19).

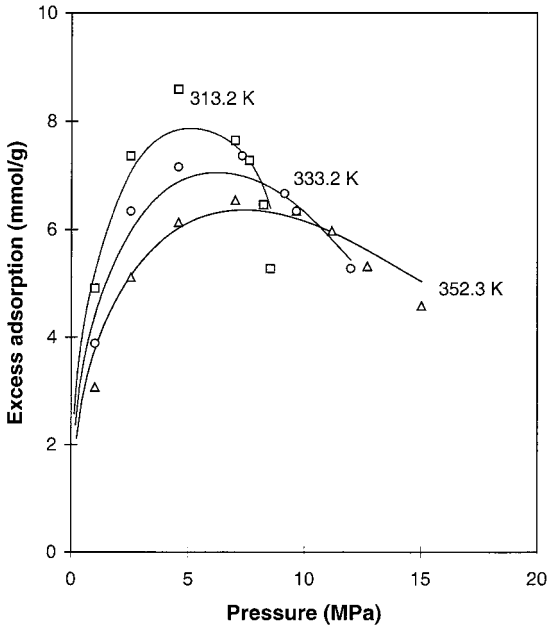

Figure 18. Adsorption of CO_2 on ACK carbon (983 m^2/g) where $H = 15.4$ Å and $\epsilon_{fs}/k = 109$ K. Data of Ozawa et al. (ref 22).

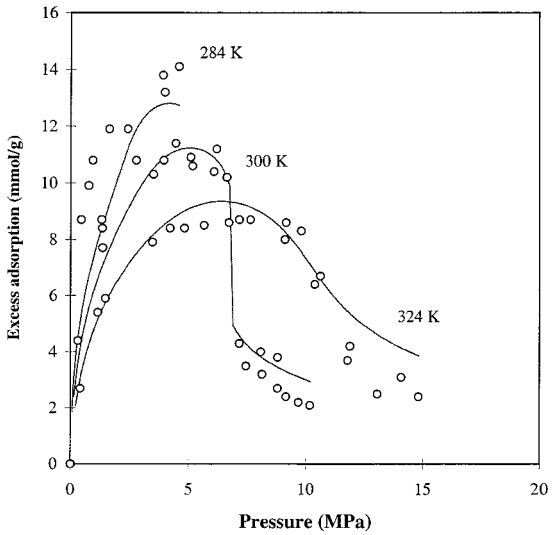

Figure 17. Carbon dioxide adsorption on DeGussa IV (1699 m^2/g) where $H = 15.5$ Å and $\epsilon_{fs}/k = 77$ K. Data of Chen et al. (ref 13).

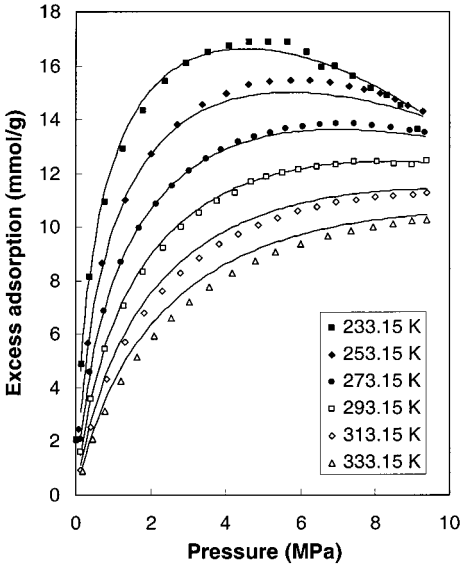

Figure 19. Adsorption of methane on activated carbon (AX-21) where $H = 11.7$ Å and $\epsilon_{fs}/k = 59$ K. Data of Zhou et al. (ref 10).

Our goal is to fine-tune the approach to make it amenable for use in process simulation software with multicomponent systems. Further work in this area would involve looking at the adsorption of mixtures, for example,

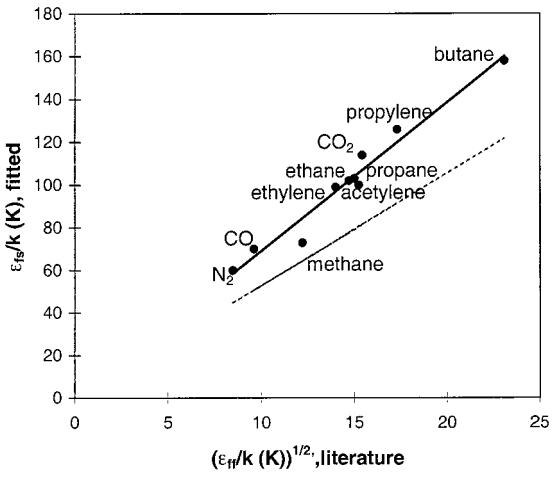

Figure 20. Correlation of fluid−solid parameters and the Lennard-Jones parameter of the adsorbate. L-J parameters are from Reid et al. (ref 18). Dashed line: L−B rule.

the prediction and modeling of azeotropic adsorption. We would like to extend the ESD to modeling of zeolites. Also, more work needs to be done with hydrogen-bonding fluids such as water, as our efforts in applying the ESD in this particular area are not yet quantitative.[26] Supercritical fluid adsorption is another subject of immediate interest because adsorption isotherms exhibit crossovers that can be represented with the SLD approach. Code used for fitting isotherms with the ESD−SLD model can be downloaded from the Home Page link at www.egr.msu.edu/∼lira.

Acknowledgment. We express appreciation to J. Richard Elliott for sharing the ESD code which was adapted for modeling and also acknowledge the MSU Crop and Bioprocessing Center for support of Cassandra Smith and Aaron Soule.

(26) Smith, C. A. Adsorption of Water on Carbon: A Study Using the ESD Equation of State. Master's Thesis, Michigan State University, East Lansing, MI, 1997.

Nomenclature

A	surface area per unit weight of adsorbent
a	Peng−Robinson attractive energy parameter
b	ESD size parameter
c	ESD shape factor
Eta	dimensionless distance from first wall in slit model/fluid−solid diameter
f	fugacity
H	distance from carbon center to carbon center across slit
k	Boltzmann's constant
P	pressure
q	ESD shape factor
R	gas constant
T	temperature
Xi	dimensionless distance from second wall in slit/fluid−solid diameter
Y	ESD attractive energy parameter
z	distance from the surface of adsorbent
Z	compressibility factor

Greek

α	spacing between carbon planes
ϵ	interaction parameter
η	reduced density = $b\rho$
ρ	density
σ	molecular diameter
Γ^{ex}	excess
Ψ	fluid−solid potential

Superscripts

attr	attractive term
LCL	local property
rep	repulsive term

Subscripts

bulk	property of bulk fluid
ff	fluid−fluid property
fs	fluid−solid property

LA000311N